

SEISMIC RESPONSE OF STRUCTURES BURIED PARTIALLY IN A MULTI-LAYERED SOIL MEDIUM

by

T. Abe^I and A. H-S. Ang^{II}

SYNOPSIS

A method for evaluating the response of structure-soil systems to specified bedrock seismic motions is presented. Structures can be partially buried in a multi-layered viscoelastic soil medium overlaying a hard base (e.g., bedrock); the effect of the surrounding soil pressures, and both rocking and translational motions of the structure, are included. The required response of the coupled structure-soil system is calculated numerically using a fast Fourier transform algorithm⁽¹⁾; solutions represent the three-dimensional response of the coupled system, and results are useful for design consistent with current specification of local motion intensity.

INTRODUCTION

The response of a structure to earthquake ground motions is a three-dimensional problem involving a coupled structure-soil system subjected to a complex history of ground excitation during the passage of the seismic waves. For engineering purposes, the local ground motions are usually assumed to consist of shear waves propagating upward from the bedrock. Amplifications of the waves and resulting structure-soil interactions are determined by idealized one-dimensional analysis, or by two-dimensional finite-element analysis. One-dimensional analysis is clearly a gross idealization of the complex interaction phenomenon whereas any finite-element analysis is costly and neglects the effects of the third spatial dimension.

The seismic response of a three-dimensional coupled structure-soil system consisting of a cylindrical structure embedded fully in a viscoelastic, homogeneous soil stratum subjected to bedrock shear waves has been solved by Tajimi⁽⁵⁾; similar problems have also been examined by other Japanese authors^{(2) (3) (4)}. The original method of Tajimi is extended here to consider cylindrical structures partially embedded in a multi-layered viscoelastic medium overlaying a hard base; a prototype system would be a nuclear reactor containment vessel.

The method can be used to evaluate the coupled response of structure-soil systems to specified bedrock earthquake motions; results are useful for design purposes, consistent with current specification of site-intensity (i.e., in terms of peak horizontal accelerations at the bedrock level).

^IStructural Engineer and Research Engineer, Gilbert Associates, Inc., Reading, Penna., U.S.A.

^{II}Professor of Civil Engineering, University of Illinois at Champaign-Urbana, Urbana, Illinois, U.S.A.

ASSUMPTIONS AND PROCEDURE

Consider a structure buried to a depth h in a linearly viscoelastic soil medium with total thickness H overlying a very hard base; e.g., bedrock. There is a significant difference in hardness between the base and the overlying material. A general sketch of the system is shown in Fig. 1. The hard base is considered as a rigid half-space, and any earthquake-type input motion will be specified horizontally at this base in the x - z plane in Fig. 1.

It is assumed that a structure will consist of a flexible above-ground structure with single-degree-of-freedom and a rigid cylindrical below-ground structure with radius r_0 and height H_0 . The center of gravity of the below-ground structure is indicated by G . H_g is defined by the distance between the center of rocking and swaying of the below-ground structure (indicated by S in Fig. 1) and the hard base. H_g is always constant; in other words, there will be no vertical motion of the structure. Theoretically, the system is a three-dimensional problem.

Basic assumptions are as follows: (1) bedrock is subjected to horizontal motions only; (2) the free field motion of the soil medium is described by one dimensional wave propagation theory; (3) the soil medium is layered and linearly viscoelastic described by a Voigt-type model; (4) the interaction effect on the bottom of the structure and that on the side-wall of the structure are uncoupled in the frequency domain as shown in Fig. 2.

The solution starts with the hard base subjected to a harmonic horizontal motion x_g ,

$$x_g = u_g e^{i\omega t} \dots\dots\dots(1)$$

where u_g = displacement amplitude of the motion, $i = \sqrt{-1}$, ω = circular frequency, and t = time. Once the harmonic response of the system is obtained, the frequency response function (the transfer function) can be generated. Since the system is frequency-dependent, the Fourier transformation technique is used to obtain the transient structural response.

DYNAMIC PRESSURE BY SURROUNDING SOIL

Tajimi ⁽⁵⁾ solved the dynamic pressures of the surrounding soil on a cylindrical structure in a viscoelastic stratum when the structure moved in a rocking-translational mode subjected to a fixed center of rotation S located on a rigid half-space which was under specified horizontal motions. The bottom part of the embedded structure was assumed to be in direct contact with the bedrock; accordingly, the effects of amplification in the intervening soil strata are neglected. Also, any dynamic soil pressure on the structure is induced by the rocking motion only.

In the present study the soil medium is assumed to be layered and a rigid portion of a structure is partially buried in the medium. The partially embedded structure undergoes both translational and rocking

motions which are different from the bedrock horizontal motions; the dynamic soil pressures, therefore, are due to horizontal and rocking motions of the structure. The governing equations of motion, when the hard base is subjected to a harmonic motion of Eq. (1), can be expressed in the matrix form in cylindrical coordinates as follows:

$$\left[\begin{array}{c|c} (\lambda_m + 2\mu_m) \frac{\partial}{\partial r} & -\mu_m \frac{1}{r} \frac{\partial}{\partial \theta} \\ \hline (\lambda_m + 2\mu_m) \frac{1}{r} \frac{\partial}{\partial \theta} & \mu_m \frac{\partial}{\partial r} \end{array} \right] \left\{ \frac{\Delta_m}{2\bar{\omega}_{z,m}} \right\} =$$

$$\left(\rho_m \frac{\partial^2}{\partial t^2} - \mu_m \frac{\partial^2}{\partial z^2} - \mu'_m \frac{\partial^3}{\partial t \partial z^2} \right) \left\{ \frac{u_m}{v_m} \right\} + \rho_m u_g \omega^2 e^{i\omega t} \left\{ \frac{-\cos \theta}{\sin \theta} \right\} \dots (2)$$

for $H_{m,m} \leq z \leq H_{m,m-1}$, and $m = 1, 2, 3, \dots, N$. In Eq. (2) u_m, v_m = relative horizontal displacement of the m (th) layer in the r and θ directions respectively; N = total number of layers, Δ_m = dilatation, $2\bar{\omega}_{z,m}$ = rotation in the x - y plane, λ_m, μ_m = Lamé constants, μ'_m = viscosity constant; and ρ_m = soil density.

The boundary conditions are; (1) $v_m = 0$ for $\theta = 0$ and π , (2) $u_m = 0$ for $\theta = \pi/2$ and $3\pi/2$, (3) continuity of displacement along the boundaries of the below-ground structure and the medium, (4) $\sigma_{r,m} = \sigma_{\theta,m} = \tau_{r\theta,m} = 0$ for $r = \infty$; where

$$\sigma_{r,m} = \lambda_m \Delta_m + 2\mu_m \frac{\partial u_m}{\partial r}$$

$$\sigma_{\theta,m} = \lambda_m \Delta_m + 2\mu_m \left(\frac{1}{r} \frac{\partial v_m}{\partial \theta} + \frac{u_m}{r} \right)$$

$$\tau_{r\theta,m} = \mu_m \left(\frac{1}{r} \frac{\partial u_m}{\partial \theta} + \frac{\partial v_m}{\partial r} - \frac{v_m}{r} \right)$$

(5) $u_N = v_N = 0$ for $z = 0 = H_{N,N}$; (6) $\tau_{zr,1} = \tau_{z\theta,1} = 0$ for $z = H = H_{1,0}$ where

$$\tau_{zr,m} = \tilde{\mu}_m \frac{\partial u_m}{\partial z}$$

$$\tau_{z\theta,m} = \tilde{\mu}_m \frac{\partial v_m}{\partial z}$$

$$\tilde{\mu}_m = \mu_m + \mu'_m \frac{\partial}{\partial t};$$

and (7) continuity of displacement and shearing stress along the horizontal boundaries between two adjacent layers.

The solutions of Eq. (2) can be expressed as Eq. (3) by superposing the homogeneous solutions $*u_m, *v_m$ and the particular solutions $**u_m, **v_m$:

$$\left. \begin{array}{l} u_m = *u_m + **u_m \\ v_m = *v_m + **v_m \end{array} \right\} \dots \dots \dots (3)$$

When r increases to infinity, both dilatation and rotation will diminish.

The equations to be solved are as follows:

$$\left(\rho_m \frac{\partial^2}{\partial t^2} - \mu_m \frac{\partial^2}{\partial z^2} - \mu'_m \frac{\partial^3}{\partial t \partial z^2} \right) \left\{ \frac{*u_m}{**v_m} \right\} = -\rho_m u_g \omega^2 e^{i\omega t} \left\{ \frac{-\cos \theta}{\sin \theta} \right\} \dots (4)$$

for $H_{m,m} \leq z \leq H_{m,m-1}$, $1 \leq m \leq N$.

The solutions of Eq. (4) are a combination of the particular solution $**u_m^{(p)}, **v_m^{(p)}$ and the homogeneous solutions $*u_m^{(h)}, *v_m^{(h)}$.

The particular solutions can be obtained by modifying Tajimi's solutions, yielding

$$\left. \begin{aligned} \left\{ \begin{array}{l} **u_m^{(p)} \\ **v_m^{(p)} \end{array} \right\} &= \sum_{m=1}^{\infty} \beta_{m,n} \sin \frac{(2n-1)\pi z}{2H} u_g \omega^2 e^{i\omega t} \left\{ \begin{array}{l} \cos \theta \\ -\sin \theta \end{array} \right\} \\ \left\{ \begin{array}{l} **u_m^{(h)} \\ **v_m^{(h)} \end{array} \right\} &= (A_m e^{i\alpha_m z} + B_m e^{-i\alpha_m z}) u_g \omega^2 e^{i\omega t} \left\{ \begin{array}{l} \cos \theta \\ -\sin \theta \end{array} \right\} \end{aligned} \right\} \dots\dots\dots (5)$$

where

$$\begin{aligned} \alpha_m &= \omega / C_{S,m} \xi_m \\ \xi_m &= \sqrt{1 + i \omega \mu'_m / \mu_m} \\ \beta_{m,n} &= \frac{2}{(2n-1)\pi} \left(\frac{1}{\omega_{g,m} \xi_{m,n}} \right)^2 \\ \omega_{g,m} &= C_{S,m} \pi / 2 H_m \\ \xi_{m,n} &= \sqrt{(2n-1)^2 (1 + 2i \frac{\omega}{\omega_{g,m}} h_{g,m}) (\frac{H_m}{H})^2 - (\frac{\omega}{\omega_{g,m}})^2} \\ h_{g,m} &= \frac{\omega_{g,m} \mu'_m}{2 \mu_m} \\ C_{S,m} &= \sqrt{\mu_m / \rho_m} \end{aligned}$$

A_m and B_m are unknown constants (but frequency dependent) which are determined from the boundary conditions; specifically boundary conditions (5), (6) and (7). A well-known procedure, attributed to Haskell⁽⁶⁾, can be applied to get A_m and B_m . Details of derivation can be found in Reference 7.

The homogeneous solutions $*u_m$ and $*v_m$ should satisfy the following equations;

$$\left[\begin{array}{c} (\lambda_m + 2\mu_m) \frac{\partial}{\partial r} \left| -\mu_m \frac{1}{r} \frac{\partial}{\partial \theta} \right. \\ (\lambda_m + 2\mu_m) \frac{1}{r} \frac{\partial}{\partial \theta} \left| \mu_m \frac{\partial}{\partial r} \right. \end{array} \right] \left\{ \begin{array}{c} \Delta_m \\ 2 \omega_{z,m} \end{array} \right\} = \left(\rho_m \frac{\partial^2}{\partial t^2} - \mu_m \frac{\partial^2}{\partial z^2} - \mu'_m \frac{\partial^3}{\partial t \partial z^2} \right) \left\{ \begin{array}{c} *u_m \\ *v_m \end{array} \right\} \dots\dots\dots (6)$$

for $H_{m,m} \leq z \leq H_{m,m-1}$ and $1 \leq m \leq N$.

Following identically the method in Reference 5, and with slight modification, the solutions for Eq. (6) are

$$\left. \begin{aligned} *u_m &= \cos \theta e^{i\omega t} \left\{ \sum_{n=1}^{\infty} \sin \frac{(2n-1)\pi z}{2H} \left[-C_{m,n} \left(\frac{1}{r} K_1(rq_{m,n}) \right) \right. \right. \\ &\quad \left. \left. + q_{m,n} K_0(rq_{m,n}) \right) + D_{m,n} \frac{1}{r} K_1(rt_{m,n}) \right] \right\} \\ *v_m &= \sin \theta e^{i\omega t} \left\{ \sum_{n=1}^{\infty} \sin \frac{(2n-1)\pi z}{2H} \left[-C_{m,n} \frac{1}{r} K_1(rq_{m,n}) \right. \right. \\ &\quad \left. \left. + D_{m,n} \left(\frac{1}{r} K_1(rt_{m,n}) + t_{m,n} K_0(rt_{m,n}) \right) \right] \right\} \end{aligned} \right\} \dots\dots (7)$$

where

$$\begin{aligned} q_{m,n} &= \xi_{m,n} \omega_{g,m} / C_{d,m} \\ t_{m,n} &= \xi_{m,n} \omega_{g,m} / C_{S,m} \\ C_{d,m} &= \sqrt{(\lambda_m + 2\mu_m) / \rho_m} \\ K_0 \quad \text{and} \quad K_1 &= \text{Modified Bessel Function of the second kind of order zero and one, respectively.} \end{aligned}$$

$C_{m,n}$ and $D_{m,n}$ are frequency dependent (unknown) constants. These are to be determined by boundary condition (3).

Let x_S and ϕ be respectively the relative horizontal translation between the structure and the hard base, and the absolute rotation of the below-ground portion of the structure. Displacement of a point on the surface of the sub-structure can be written as

$$\begin{Bmatrix} u \\ v \end{Bmatrix} = \sum_{n=1}^{\infty} \left\{ x_S + \phi(z-H_S) \right\} \frac{4}{(2n-1)\pi} \sin \frac{(2n-1)\pi z}{2H} e^{i\omega t} \begin{Bmatrix} \cos \theta \\ -\sin \theta \end{Bmatrix} \quad (8)$$

for $r = r_0$ and $H_B \leq z \leq H$. Since displacements of the medium are also obtained from Eq. (3) by letting $r = r_0$, $C_{m,n}$ and $D_{m,n}$ are obtained from Eqs. (3) and (8).

The dynamic soil pressure acting on the below-ground structure per unit length of x , $p_m(z)$, at the level z is given by

$$p_m(z) = \int_0^{2\pi} (\sigma_{r,m}|_{r=r_0} \cos \theta - \tau_{\theta,m}|_{r=r_0} \sin \theta) r_0 d\theta \quad \dots\dots\dots (9)$$

for $H_B \leq z \leq H$, and $H_{m,m} \leq z \leq H_{m,m-1}$. It can be shown⁽⁷⁾ that the particular solutions u_m and v_m do not contribute to $p_m(z)$.

Finally the total dynamic soil pressure acting on the structure can be obtained, consisting of the translational force \bar{F} and overturning moment \bar{M} in the x and ϕ direction, respectively, as follows:

$$\left. \begin{aligned} \bar{F} &= \sum_{m=1}^{\bar{m}} \int_{a_m}^{b_m} p_m(z) dz \\ &= (\bar{F}_x x_S + \bar{F}_\phi \phi - \bar{F}_i u_g \omega^2) e^{i\omega t} \\ \bar{M} &= \sum_{m=1}^{\bar{m}} \int_{a_m}^{b_m} (z - H_S) p_m(z) dz \\ &= (\bar{M}_x x_S + \bar{M}_\phi \phi - \bar{M}_i u_g \omega^2) e^{i\omega t} \end{aligned} \right\} \dots\dots\dots (10)$$

where $H_{\bar{m},\bar{m}} \leq H_B < H_{\bar{m},\bar{m}-1}$, $a_m = H_{m,m}$, $b_m = H_{m,m-1}$, $a_{\bar{m}} = H_B$, and $b_{\bar{m}} = H_{\bar{m},\bar{m}-1}$.

INTERACTION EFFECT ON THE BOTTOM OF STRUCTURE

The interaction effects, besides the dynamic soil pressure, are the translation P and rotation M at the bottom of the structure. The translational component P can be obtained exactly by integrating shearing the stresses distributed over the bottom surface;

$$P = \int_0^{r_0} \int_0^{2\pi} (\tau_{rz} \cos \theta - \tau_{\theta z} \sin \theta) r d\theta dr \quad \dots\dots\dots (11)$$

at $z = H_B$. Eq. (11) gives the dynamically coupled interaction force with the dynamic soil pressures.

Recalling assumption (5), P and M can be obtained approximately by the force-displacement relationship which is defined by the ratio of the excitation force of a mass-less foundation on the half-space to the complex displacement in the same direction of the force in the frequency

domain. The effect of the burial depth h on the force-displacement ratio is not considered.

Kobori and Suzuki⁽⁸⁾ studied foundation vibration on multi-layered viscoelastic media. Their study of two-layered media showed that if the thickness of the top layer was at least twice the width of a foundation disk the force-displacement ratio became similar to that of a half-space system. Most practical cases of interest satisfy this condition.

The equivalent mechanical model for the force-displacement ratio is often expressed by the Voigt type system. Consequently, two springs K_x , K_ϕ and two dash-pots C_x , C_ϕ are used as shown in Fig. 3. These mechanical constants are frequency dependent and are approximated by adequate polynomial forms based on the numerical values listed in References 9 and 10 for the foundation vibration on nonviscous and viscous half-space soil media with Poisson ratio of $\frac{1}{4}$.

APPLICATION OF THE LINEAR MODEL

A summary of certain experimental studies is reported in Reference 11. Three small scale rigid structures built of reinforced concrete were used in the experiment. The structures were embedded partially in the ground at three different locations. Simultaneous observations of earthquake motions were obtained not only at parts of the structure, but at several locations in the ground with different under-ground levels. Since the raw data of recorded accelerograms were not available to the public, the accelerograms used in this study were recreated from the published records reported in Reference 11.

The linear system idealized for this study consists of a five-layer soil stratum, coupled with a rigid cylinder which is equivalent to the model structure of Reference 11. The model structure is reported to have behaved like a rigid body during earthquake motion. The location of the center of translation and rotation S was assumed to be at the base of the structure. The location of the hard base was assumed to be at a depth of 69.0 ft. from the ground surface. Soil properties are listed in Table 1 and are shown in Fig. 4. Structural properties are; $r_0 = 6.48$ ft., H_0 (height) = 35.18 ft., and weight = 178.20 kips.

The response spectra of the recreated earthquake records obtained for zero damping are plotted in Fig. 5 on a tripartite plot.

It was assumed that viscous damping includes both the damping in the soil media and that due to impedance ratio between the soil and the bed-rock. The viscosity coefficients used in the calculations are listed in Table 1.

Response spectra at different locations in the soil medium and the structure are shown in Figs. 6 through 8. The observed and calculated spectra are in close agreement. On the basis of this comparison, the applicability of the proposed approach to practical problems of structure-soil interaction appears to be confirmed.

LIMITED PARAMETER STUDIES

The structure-soil system for the parameter study is composed of soil layers and a rigid cylindrical structure to which a damped single-degree-of-freedom oscillator (SDF) is connected, as shown in Fig. 3. A prototype structure of the model would be a containment vessel in a nuclear power plant. Prime interest of the study is the base shear or the relative distortion of the SDF.

Two sets of linear solutions are considered as shown in Fig. 9; one consists of a SDF system with five layers of soil, and the other with four layers of soil. Soil and structure properties and numerical values of the parameters follows; $f_y = 2.5 \sim 25$ (cps), $M_f = 2350 \sim 23500$ (kips), $\xi = .0025 \sim .015$, $M_y/M_f = .25$, $M_f/M_{soil} = .115 \sim 1.15$, $h/r_o = 1 \sim 2$, $r_o/C_{s, \bar{m}+1} = .012 \sim .024$, and $\omega_y/\omega_g = .236 \sim 4.25$ where f_y = fundamental frequency of the SDF, M_y and M_f are masses of the SDF and the sub-structure, respectively; ξ = the critical damping ratio of the SDF, and ω_g = dominant frequency of the soil medium.

The Taft accelerogram (1952 S69E component) was applied at the bed-rock level as an input excitation. In Fig. 10 the relationship between maximum relative distortion $\text{Max}(Y)$ and ω_y is plotted. There is no significant difference in $\text{Max}(Y)$ between the unbackfilled case and backfilled case. The four-layer system produces a larger $\text{Max}(Y)$ than the five-layer system due to a greater amplification of the ground at the depth h . The effect of the structure-soil mass ratio (M_f/M_{soil}) was examined, where was kept constant at 20 rad./sec. which was close to one of the dominant frequencies of the ground. $\text{Max}(Y)$ is plotted in Fig. 11. The computed results show that the unbackfilled case is more sensitive to the structure-soil mass ratio than the backfilled case which includes the dynamic side pressures.

CONCLUSIONS

The following conclusions may be made based on the studies performed herein:

(1) The surrounding soil is significant in contributing to the structural response of a class of structures with massive weight and low height. This effect has both a driving effect and a confining effect on the structural response. The former effect increases response of the structure and the latter effect decreases it. These two opposing effects contribute to the structural response in a complicated manner.

(2) Neglecting the effects of the surrounding soil may not always be a conservative assumption, as far as the maximum relative distortion of a structure is concerned; generally, however, these effects tend to reduce the maximum relative distortion of a structure.

(3) Replacement of the inertial effect of the surrounding soil by the so-called "inertial soil mass" is not recommended for a deeply buried structure, because the inertial effect of the surrounding soil is highly

frequency dependent.

(4) In the current practice of aseismic design of a nuclear power plant facility, the predicted design base earthquake motions are defined by the peak acceleration, smooth response spectra, and associated time histories of accelerations for different percent of critical damping. Generally, the response spectra is specified at both bedrock and ground surface. The ground surface response of a power plant site varies from one building location to another because of the influence of the overlaying soil profile. This would provide a justification for a seismic analysis using smooth response spectra and associated time history input defined at the bedrock level. In this approach structure-soil interaction can be reasonably included in a dynamic analysis of each building or possibly a three dimensional dynamic analysis of an entire power plant facility. With this in mind, the bedrock-soil-structure system developed herein is practically useful when the input motion is specified at the bedrock level. The proposed approach can be applied for the practical purpose of determining the major effects of structure-soil interaction.

ACKNOWLEDGEMENT

The use of the computer facilities at Gilbert Associates, Inc. is gratefully acknowledged. Encouragement of Mr. D. K. Croneberger, Chief Structural Engineer, to the first author is also appreciated.

BIBLIOGRAPHY

1. Cooley, J. W., and Tukey, J. W., "An Algorithm for the Machine Calculation of Complex Fourier Series", Mathematics of Computation, Vol. 19, No. 99, April 1965, pp. 297-301.
2. Goto, H., and Akiyoshi, T., "Seismic Response Characteristics of Foundation Structures in Elastic Ground, (Rigid Foundation Structures with Elliptic Cross Section)", Proceedings of the Japan Society of Civil Engineers, No. 177, May 1970, pp. 21-32, (Japanese).
3. Toki, K., "Seismic Response of Structure in Heterogeneous Ground", Proceedings of the Third Japan Earthquake Engineering Symposium, Nov. 1970, Tokyo, Japan, pp. 73-80 (Japanese).
4. Yasui, Y., and Nakagawa, K., On the Vibration of Embedded Rigid Structure Having Sway-Rocking Vibration Freedom. The Technical Research Institute, Ohbayashi-gumi Ltd., July 1972.
5. Tajimi, H., "Dynamic Analysis of a Structure Embedded in an Elastic Stratum", Proceedings of the Fourth World Conference on Earthquake Engineering, Santiago, Chile, January 1969.
6. Haskell, N. A., "The Dispersion of Surface Waves on Multi-layered Media", Bulletin of the Seismological Society of America, Vol. 43, 1953, pp. 17-34.
7. Abe, T., "Seismic Response of a Linear Bedrock-Soil-Structure Interaction System", Ph.D. Thesis, Department of Civil Engineering, University of Illinois, Urbana, Illinois, 1972.

8. Kobori, T., and Suzuki, T., "Foundation Vibrations on a Viscoelastic Multi-Layered Medium", Proceedings of the Third Japan Earthquake Engineering Symposium, November 1970, Tokyo, Japan, pp. 493-500.
9. Kobori, T., Minai, R., Suzuki, T., and Kusakabe, K., "Dynamical Ground Compliance of Rectangular Foundation on a Semi-Infinite Elastic Medium", Bulletin of the Disaster Prevention Research Institute, Kyoto University, Kyoto, Japan, Vol. 10A, March 1967 (Japanese).
10. Kobori, T., Minai, R., Suzuki, T., and Kusakabe, K., "Dynamical Ground Compliance of Rectangular Foundation on a Semi-Infinite Visco-Elastic Medium", Bulletin of the Disaster Prevention Research Institute, Kyoto University, Kyoto, Japan, Vol. 11A, March 1968 (Japanese).
11. Experimental Studies on the Vibrational Characteristics of the Nuclear Power Plant Facilities under Earthquake Motions. Report, Architectural Institute of Japan, March 1968 (Japanese).

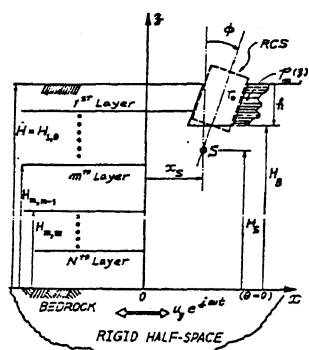


FIGURE 1.
DESCRIPTION OF THE
PROBLEM

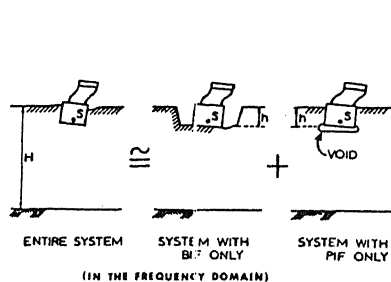


FIGURE 2.
SUPERPOSITION OF TWO
SYSTEMS

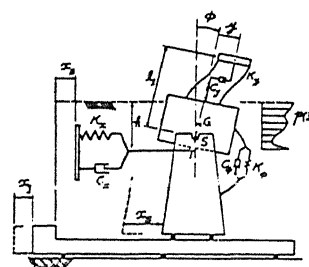


FIGURE 3.
BEDROCK-SOIL-STRUCTURE
INTERACTION SYSTEM

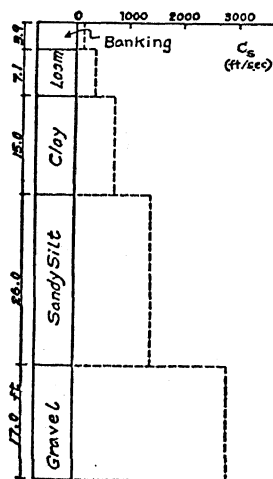


FIGURE 4.
SHEAR WAVE VELOCITIES
FOR THE LINEAR MODEL

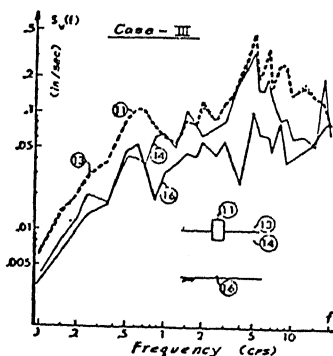


FIGURE 5.
RESPONSE SPECTRA
(CASE-3)

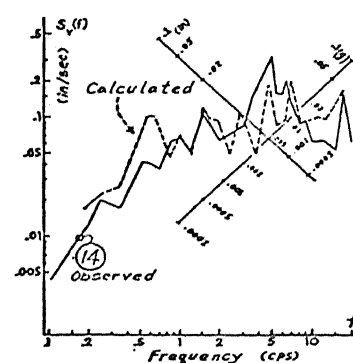


FIGURE 6.
RESPONSE SPECTRA
(INSIDE GROUND)

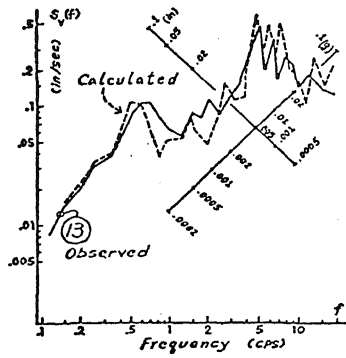


FIGURE 7.
RESPONSE SPECTRA
(GROUND SURFACE)

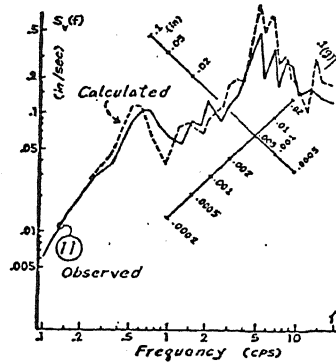


FIGURE 8.
RESPONSE SPECTRA
(STRUCTURE TOP)

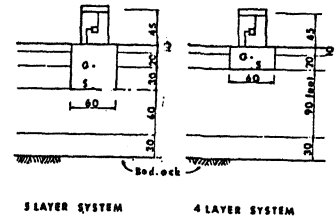


FIGURE 9.
5 LAYER SYSTEM AND
4 LAYER SYSTEM

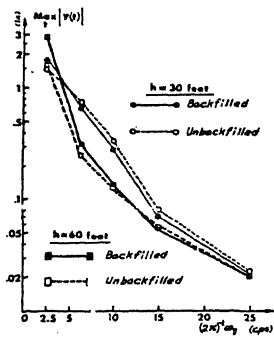


FIGURE 10.
MAXIMUM RELATIVE DIS-
PLACEMENT AND FUNDA-
MENTAL FREQUENCY

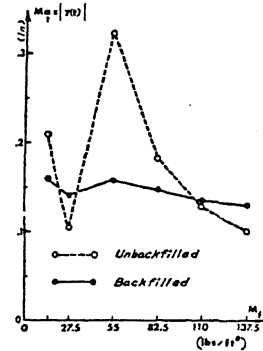


FIGURE 11.
EFFECT OF STRUCTURE-
SOIL MASS RATIO

TABLE 1. SOIL PROPERTIES

Layer	ρ_m	C_u	C_d	H_m	h_g
1	70	80	108	3.9	.129
2	70	300	586	7.1	.265
3	110	721	1410	15.0	.159
4	125	1410	2460	26.0	.174
5	125	2800	4900	17.0	.259

Layer	M_s^*/M_f	$\omega_{s,n}$
1	.004	32.21
2	.004	66.34
3	.002	75.46
4	.002	85.19
5	.001	258.72

TABLE 2a. SOIL PROPERTIES (5 LAYERS)

No. of Layer	H_m (ft)	Soil Classification	$C_{s,m}$	$C_{d,r}$	ρ_m	$h_{g,m}$	$\omega_{s,m}$	μ^*/μ_m
1	10	Sand	300	625	70	.0236	47.12	.0010
2	20	Sand	500	1041	90	.0176	32.27	.0009
3	30	Sand	800	1652	110	.0157	21.89	.0008
4	60	Gravel	2500	5216	130	.0164	62.45	.0005
5	30	Silt Stone	3500	7296	130	.0450	181.26	.0005

TABLE 2b. SOIL PROPERTIES (4 LAYERS)

No. of Layer	H_m (ft)	Soil Classification	$C_{s,m}$	$C_{d,r}$	ρ_m	$h_{g,m}$	$\omega_{s,m}$	μ^*/μ_m
1	10	Sand	300	625	70	.0236	47.12	.0010
2	20	Sand	500	1041	90	.0176	32.27	.0009
3	90	Gravel	2500	5216	120	.0131	41.63	.0005
4	30	Silt Stone	3500	7296	130	.0450	181.26	.0005